Toward a Practical, Two-Step Process for Molnupiravir: Direct Hydroxamination of Cytidine Followed by Selective Esterification

Dinesh J. Paymode, N. Vasudevan, Saeed Ahmad, Appasaheb L. Kadam, Flavio S.P. Cardoso, Justina M. Burns, Daniel W. Cook, Rodger W. Stringham, and David R. Snead*

Read Online

ACCESS | Metrics & More | Article Recommendations | Supporting Information

ABSTRACT: A two-step synthesis of molnupiravir (**1**) is presented. This work focuses on the development of practical reaction and purification conditions toward a manufacturing route. The sequence commences from highly available cytidine (**2**), and molnupiravir is formed through direct hydroxamination of the cytosine ring and esterification of the sugar's primary alcohol without use of protecting or activating groups. A highly crystalline hydrate of N-hydroxycytidine (**3**) resulted in an easily purified intermediate, and a practical, off-the-shelf enzyme was selected for the acylation. The yield was increased through a chemically promoted, selective ester cleavage, which converted a byproduct, molnupiravir isobutyryl oxime ester (**4**), into the final API. Both reactions proceed in >90% assay yield, and crystallization procedures are used to afford intermediates and active pharmaceutical ingredients in purities above 99% with an overall yield of 60%. Excellent throughput and sustainability are achieved by limiting the total concentration to 7 volumes of solvent in the course of the two reactions with an overall PMI of 26 including work-up and isolation. Environmentally friendly solvents, water and 2-methyl tetrahydrofuran, enhance sustainability of the operation.

KEYWORDS: *antiviral, molnupiravir, biocatalysis, nucleoside*

INTRODUCTION

Molnupiravir (also known as EIDD-2801 and MK-4482) is emerging as a drug candidate of increasing interest based on its potential to treat COVID-19. Molnupiravir is currently under investigation in Phase II and III clinical trials after Merck licensed the compound from Ridgeback Biotherapeutics (NCT04405570, NCT04405739, NCT04575597, and NCT04575584). Furthermore, animal studies show high promise. Molnupiravir showed broad-spectrum antiviral activity against SARS-CoV-2 with reduced virus titer in mice[1] and completely blocked SARS-CoV-2 transmission in ferrets within 24 h of administering the medication.[2] From a pragmatic standpoint, molnupiravir is orally available and is structurally simple compared to remdesivir, making future manufacture considerably less complex. There are safety concerns related to the drug, and these should be answered by the pending clinical trials.[3]

We recently disclosed synthetic routes that detailed new bond-forming steps to reach molnupiravir (Figure 1).[4] The initial synthesis[5] used for discovery purposes proceeded in 17% overall yield (yield of some steps not disclosed) over four discrete steps and sourced uridine (**5**) as the starting point rather than the more available and less expensive cytidine.[6] The newer routes sought to improve yield, decrease step-count, and select lower cost starting materials, namely, cytidine. Indeed, EIDD-2801 was made from cytidine in two steps with yields up to 75%. However, these excellent preliminary results required refinement. Intermediates and the product were isolated by column chromatography, very high enzyme loadings were employed, reactions were run under highly dilute conditions as a result of limited substrate solubility, and results were only performed at

the 1 g scale. Merck has also recently disclosed an excellent route to molnupiravir taking advantage of ribose as a starting material so as to avoid use of cytidine or uridine as a feedstock.[7]

Here, we describe the improvements to our first disclosure, which lead to a route with a favorable manufacturing profile. Understanding byproducts and the mechanism of formation allowed both reactions to reach yields of 90% in solution. Ultimately, overall isolated yield was improved by 23% (60 from 37%) with the product isolated by crystallization rather than chromatography. Solvent consumption during the course of the reaction was reduced 10-fold (7 from 68 volumes) with only 26 volumes of solvent used including work-up and isolation, and environmentally preferred solvents were selected (water and 2-methyltetrahydrofuran). An "off-the-shelf" enzyme (CAL-B) performed the acylation, and enzyme loading was reduced 10-fold (200 → 20 wt %). Reactions were scaled to 500 g (NHC) and 100 g (molnupiravir), and final API was generated with a purity of 99.4% with the majority of residuals being the active drug, NHC (0.6%).

A NOTE ON CYTIDINE SUPPLY

We believe that cytidine is a suitable starting point for the synthesis of molnupiravir based on its high availability at the

Discovery Route:

M4ALL Route:

	Overall Yield:	Step Count:	SM Price:[6]	Solvent Consumption (Volumes):	Enzyme Loading:	Final Step Scale:	Isolation:
Initial Synthesis	17%	4	Uridine	not determined	not applicable	6.5 g	Column
M4All 1st Gen:	37%	2	Cytidine	68	200 wt%	1 g	Column
M4All 2nd Gen:	60%	2	Cytidine	26	20 wt%	100 g	Crystallization
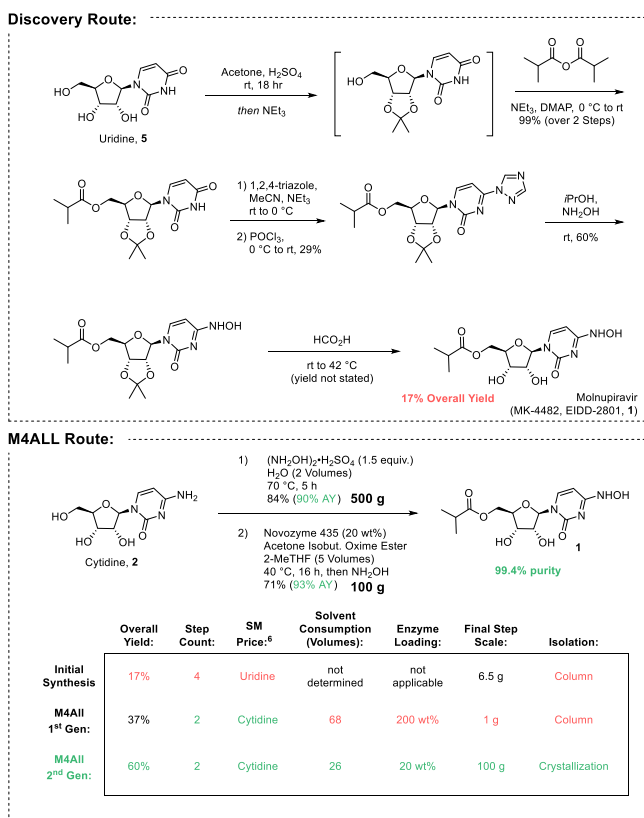
Figure 1. M4ALL's approach to molnupiravir from cytidine.

multimetric ton scale. Cytidine is an important precursor to cytidine monophosphate (**6**),[8] a compound consumed by the market in large quantity as a result of its applications in infant formula,[9] food additives,[10] and animal feed industries[11] and as a precursor to citicoline, a dietary supplement (Figure 2).[12] We proactively reached out to potential manufacturers early in our studies, and individual suppliers indicated capacity to supply ≥100 MT of cytidine.[13] Lending support to that claim, the
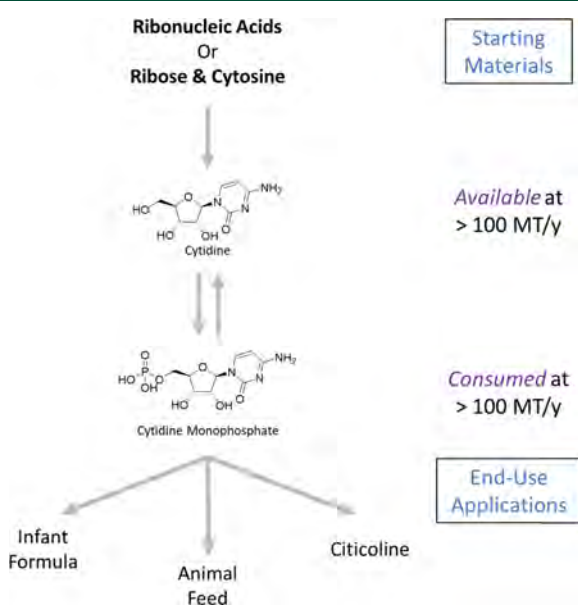

Figure 2. High volume end-use applications secures cytidine's availability.

observed volumes of cytidine monophosphate moving through the Indian import marketplace reached 62 MT in 2020, a number that in fact exceeds that of ribose (24 MT).

Cytidine production can proceed through two simple processes:

1. Recently, the single-step syntheses of both cytidine and uridine from sugars were reported. Cytidine was made enzymatically at high concentrations by combining cytosine, ribose, and a cytidine ligase.[14] Uridine was made in high yield (91%) via a chemical glycosylation of ribose with uracil promoted by phosphotungstic acid, negating the need for custom, evolved enzymes.[15] The innovator company Xianfeng Chemistry Co. (XFchem) is a large-scale supplier. Takeda simply used glucose, corn liquor, and urea to construct both cytidine[16] and uridine,[17] but the conditions were highly dilute. Significant variations of each strategy exist.

2. Classically, nucleosides are produced through digestion of natural materials, ribonucleic acids. Complete digestion results in production of the nucleosides including cytidine in quantitative yields.[8a,18] The nucleosides can be separated using ion-exchange chromatography, or the nucleoside liquor can subsequently be phosphorylated in the presence of yeast to yield the monophosphorylated nucleotides such as cytidine monophosphate.[8a–d,19] Again, many updates have ensued since the original development of this technology in the 1930s.[20]

The latent ability to supply cytidine appears to be high even though current market conditions favor consumption of the monophosphate.

■ RESULTS AND DISCUSSION

***N*-Hydroxycytidine: Reaction Screening and Impurity Profile.** In our first study, we were pleased to see that pure *N*-hydroxycytidine (**7**, NHC) could be crystallized from a concentrated reaction mixture; however, the isolated yield of the transformation was lower than desired (50%), and high solvent consumption limited material throughput.

Monitoring the reaction at a low wavelength (210 nm) revealed the presence of a second compound (**8**) in what appeared to be an otherwise clean transformation to the product (260 nm) (Figure 3). The byproduct turned out to be over-reaction of the product with a second equivalent of hydroxyl-
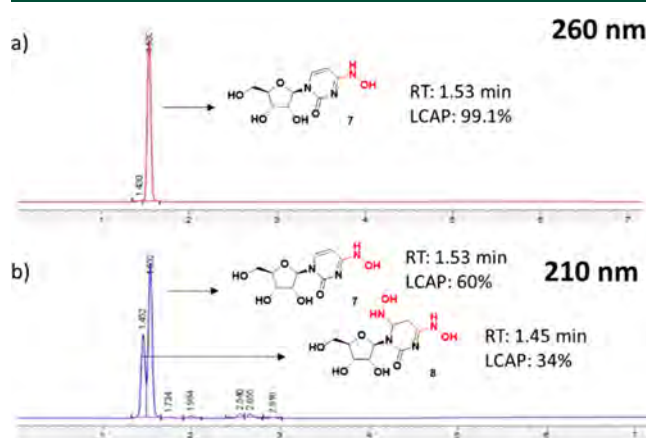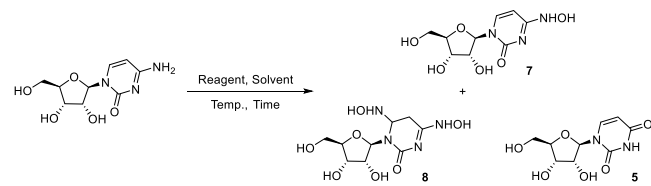

Figure 3. (a) HPLC chromatogram for the reaction at 260 nm and (b) at 210 nm.

Table 1. Optimization for Synthesis of *N*-Hydroxycytidine from Cytidine[a]

			LCAP		
entry	reagent (equiv)	solvent (vol)	7	8	5
1[b]	NH₂OH·HOAc (3)	H₂O (20 V)	60	34	
2[c]	(NH₂OH)₂·H₂SO₄ (4.5)	70% *i*PrOH in H₂O (15 V)	94		6
3[c]	(NH₂OH)₂·H₂SO₄ (0.5)	70% *i*PrOH in H₂O (2 V)	57		20

Table 1 entries: reagent/equiv and solvent values as shown.

[a]Reaction monitored at 210 nm. [b]Reaction conditions: cytidine (200 mg, 0.77 mmol), 40 °C, 48 h. [c]Reaction conditions: cytidine (200 mg, 0.77 mmol), 70 °C, 20 h.

amine, which adds to the cytosine ring in a 1,4-fashion, thus destroying the conjugated system (Table 1). This explains the compound's lower UV absorbance, and the presence of the impurity is partially a result of using an excess of hydroxylamine. Alternative conditions employing hydroxylamine sulfate in a 2-propanol/water mixture were explored. Surprisingly, cytidine was completely consumed and dihydroxamination was not observed. However, a new peak corresponding to uridine appeared in the HPLC chromatogram, revealing a second degradation pathway. Decreasing hydroxylamine sulfate equivalents exacerbated the problem.

We wondered how these impurities might be avoided. Conditions were optimized for the biphasic isopropanol/water mixture with a very high assay yield of NHC (Figure 4). The best
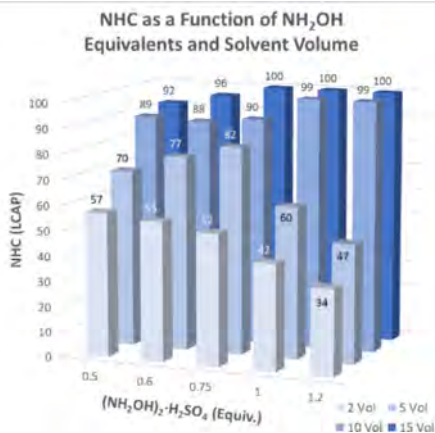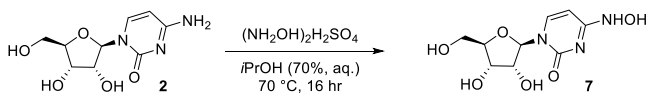

Figure 4. Optimization of transamination as a function of hydroxylamine equivalents and reaction concentration.

results were consistently obtained at 10 volumes of solvent and higher. We were pleased with the outcome but hoped for even higher concentration so as to minimize environmental impact and to maximize throughput.

We were curious how the percentage of water in isopropanol impacted the reaction (Figure 5). In pure isopropanol, hydroxamination shut down. However, water not only accelerated the reaction of cytidine but also surprisingly suppressed uridine formation. Uridine levels peaked at 10−
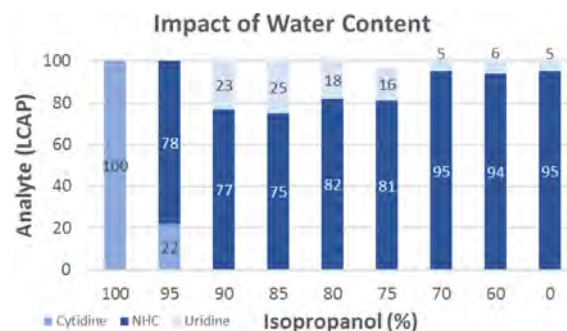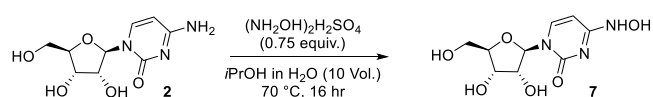

Figure 5. Reaction optimization as a function of water content in *iso*-propanol.

25% water in isopropanol. Perhaps rates of uridine and NHC formation are competitive at this cosolvent ratio.

Further probing the system showed that, in water, the reaction to form NHC could be run at much higher concentrations (Figure 6). Only 2 volumes of solvent gave results that matched those run at higher dilutions. In fact, increasing the amount of water solvent increased the levels of uridine. The reaction was
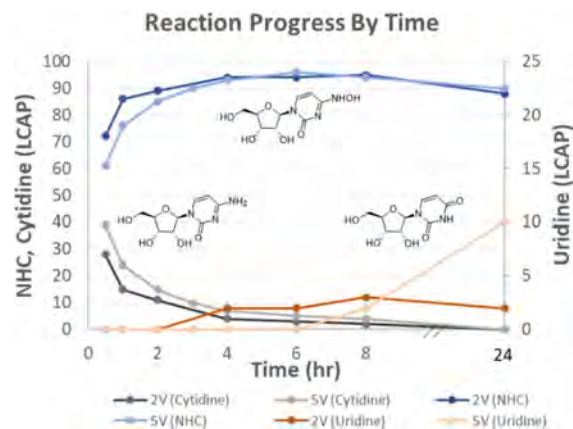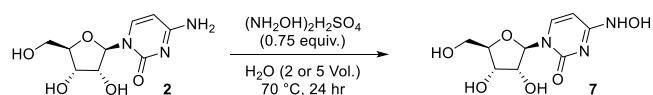

Figure 6. Transamination progress plotted as a function of time.

Table 2. 1 g Scale Reactions and Isolation of NHC[a]

| entry	(NH₂OH)₂H₂SO₄ (eqiuv)	H₂O (vol)	LCAP (cytidine/NHC)		purity (%)[b]	yield (%)[c]
			after 3 h	after 6 h		
1	0.75	2	16/84		81	70
2	0.75	5	21/79	13/87	84	82
3	1.5	2	8/92		85	84
4	1.5	5	11/89	5/95	87	82

[a]Reaction conditions: cytidine (1 g, 4.08 mmol), (NH₂OH)₂H₂SO₄, H₂O, 70 °C and time. [b]Purity assessed by qNMR. [c]Yields are adjusted to qNMR purities.

completed quickly, within 5–6 h. Allowing the reaction to run for longer times resulted in decomposition of NHC with rising levels of uridine. The presence of $NH_2OH \cdot H_2SO_4$ appears to be important in the generation of uridine. NHC or cytidine in pure water do not form **5**, unlike **3** heated in water with hydroxylamine.

N-Hydroxycytidine: Purification and Isolation of the Hydrate. We next worked to increase the scale and develop purification protocols, having optimized the reaction for maximum yield and minimal impurity formation, reaction time, and solvent consumption. Fortunately, the NHC appeared to be of limited solubility in water, which could perhaps be used for direct isolation of the product from the reaction mixture. When we increased the scale to the gram level, we noticed that the reaction started as a slurry, quickly became homogeneous (<1 h), and then again became a slurry, even at 70 °C (Table 2). To isolate the product, the reaction mixture was simply cooled to 4 °C and then filtered and washed.

Results were consistent at varying levels of hydroxylamine and solvent, but the purity of NHC was lower than expected despite the appearance of white product crystals (81–87 wt % by qNMR in DMSO-d_6). In the course of the reaction, no dihydroxamination product was observed and uridine levels were quite low. The product that crystallized directly from reaction solution contained neither impurity, and the HPLC chromatogram showed 100 LCAP (210 and 260 nm). Suspecting that hydroxylamine sulfate salts might be the culprit leading to low weight % purity, the product was recrystallized in water, yet purity did not rise above 87 wt % (qNMR). Interestingly, though the LC traces showed no other organic compounds, the ¹H NMR of NHC recorded in DMSO-d_6 showed several minor peaks accounting for 5–6% relative to the major compound (Figure 7).

This led us to wonder whether the apparent low purity was a function of NHC isomerization. Perhaps the N-hydroxycytosine can exist as a tautomer of the amine and imine. This observation would be in-line with literature precedence.[21] To explore this possibility, a variable temperature (VT) NMR experiment was carried out, increasing temperature at intervals of 10 up to 70 °C. At elevated temperatures, the minor peak disappeared and the major peak grew in intensity. Furthermore, spectra were recorded in protic media to disrupt hydrogen bonding and isomerization. Indeed, in D₂O and MeOH-d_4, the minor product was not observed. Purity increased by the amount of the minor isomer, but still, the product was only 93 wt % pure. A commercial sample of NHC was subjected to the same analysis in deuterated DMSO, water, and methanol, and the same effects were observed.
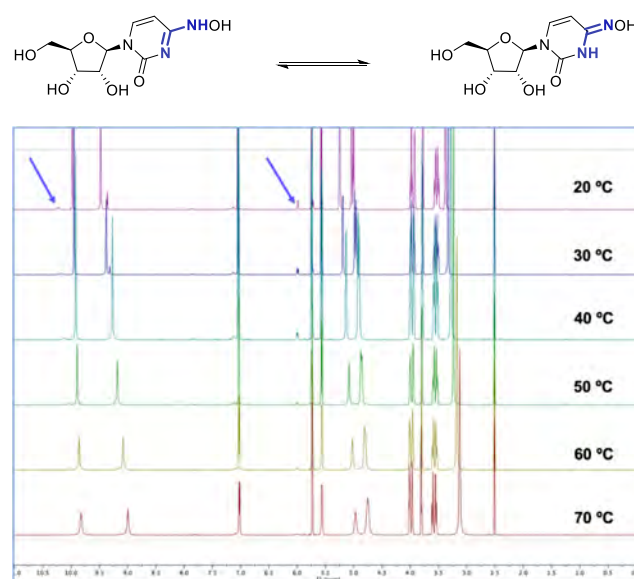
Entry	Temp. (°C)	Major isomer (%, 5.56 ppm)	Minor isomer (%, 5.98 ppm)	Combined NHC (%)
1	20	94.22	5.78	92.70
2	30	94.19	5.81	92.32
3	40	95.00	5.00	92.84
4	50	95.87	4.13	92.91
5	60	96.79	3.21	92.78
6	70	97.86	2.14	92.79

Figure 7. Variable temperature (VT) NMR spectra of NHC in DMSO-d_6 shows a minor isomer, which converts to the major isomer upon heating. The arrow in spectra points to minor isomer peaks.

We further wondered whether some inorganic material might be complexed with the sugar, accounting for the low purity, and thus, the sample was prepared for single-crystal X-ray diffraction (Figure 8). Two interesting conclusions were drawn from the X-ray analysis.

1. Water was complexed with NHC rather than inorganic metals. An intricate hydrogen-bond network formed with water's lone-pair and hydrogen atoms forming four hydrogen bonds with NHC.

2. The amine/imine tautomerization issue was observed. Interestingly, the data showed that a single hydrogen atom
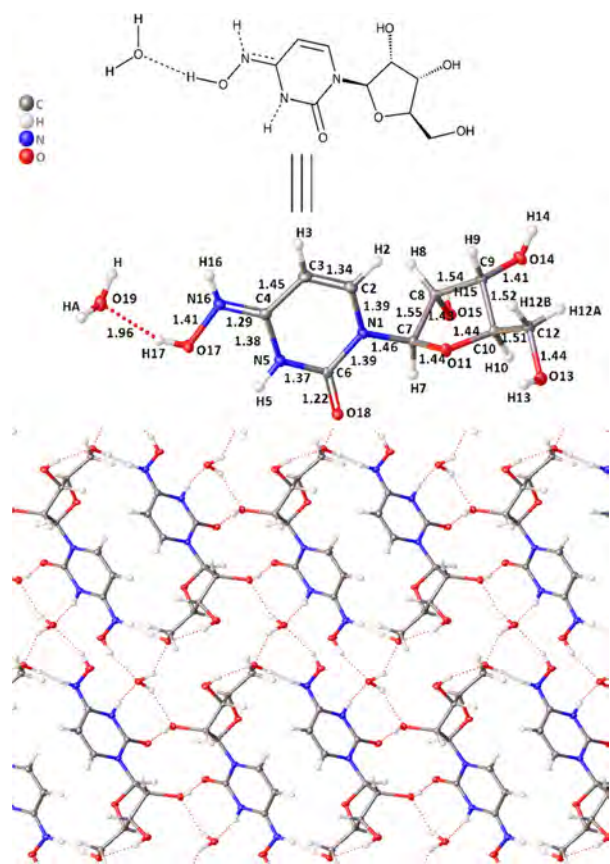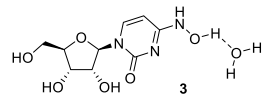
Figure 8. Single-crystal X-ray analysis shows that the hydrate of NHC is formed and suggests tautomerization.

Table 3. Reaction Performance Remains Stable upon Increasing the NHC Reaction Scale[a]

entry	scale (g)	RB flask size (mL)	time (h)	LCAP	qNMR purity	yield[b]
1	5	50	5	99.6	100	84
2	10	50	5	99.7	100	85
3	50	250	6	100	99	83
4	200	1000	6	100	100	85
5	500	2000	5	100	100	84

[a]Reaction conditions: cytidine (1 equiv), $(NH_2OH)_2H_2SO_4$ (1.5 equiv), water (2 V), 70 °C, and 5 to 6 h. [b]Yields are adjusted to qNMR purities.
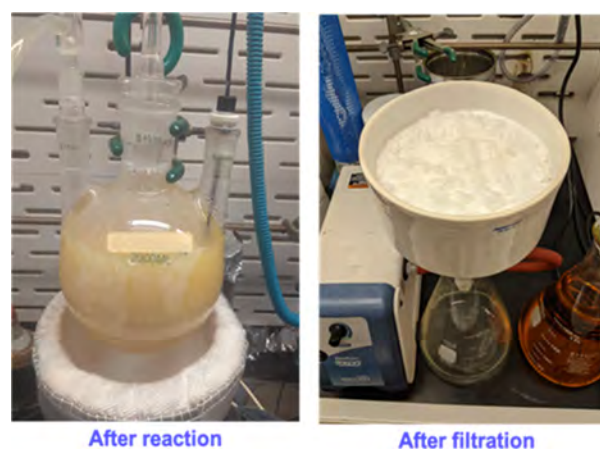
Figure 10. Image for 0.5 kg reaction to produce **3** after completion and the product after filtration.

occupied two positions at H5 and H16 in the ratio 76:24, respectively.

The seemingly low purity and unexplained mass contained in samples is reconciled by accounting for the mass of water in the molecular weight of NHC·H_2O. As the hydrate, 6.5% of sample mass is expected to be H_2O. Karl-Fischer analysis confirmed the existence of water and that it was present in the quantity predicted by the hydrate form of the intermediate (6.68 wt %) (Figure 9). From this analysis, it is concluded that the NHC is of high purity (>99%).
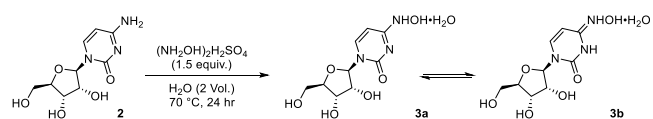

NHC MW: 259.2 g/mol
NHC·H_2O MW: 277.2 g/mol
H_2O/NHC·H_2O: 6.5%

Entry	NHC (mg)	H_2O (mg)	H_2O (%)
1	63.0	4.21	6.68
2	62.0	4.14	6.67
3	109	7.29	6.69

Figure 9. Karl-Fischer analysis confirms the presence of water.

N-Hydroxycytidine Hydrate: Scale-Up. The reaction was quickly scaled over two orders of magnitude with the knowledge that the NHC hydrate was of high purity (Table 3; Figure 10). In this manner, 500 g of intermediate **3** was made in short accord using a similar reaction setup as the smaller scale runs. These conditions increased the space−time yield to 48 g·L^{-1}·h^{-1}, a

100-fold increase from the original version. Very little change was observed across the scale (5 to 500 g), with isolated yields between 83 and 85% and purity at 99−100 wt %. Approximately 6% of NHC remained in the mother liquor for the 50 g batch, giving an overall yield of 89%. We thus feel confident that this reaction can be further scaled to the desired quantity, and this concluded our investigation into synthesis of NHC.

Molnupiravir: Reaction Optimization, Impurity Profile, and Mechanistic Analysis. In our preliminary report, we disclosed that NHC could be selectively esterified on the primary alcohol in preference to the *N*-hydroxy or secondary alcohol acylation. A number of challenges remained in order for the reaction to be pragmatically run. The maximum assays for the desired product were slightly above 80 LCAP, enzyme loading was very high (200 wt %), a large excess of 1,4-dioxane as the solvent was used (60 volumes), and the product was isolated by column chromatography.

Solvents were quickly screened, and 2-methyl THF was identified as a suitable and environmentally preferable alternative to 1,4-dioxane. Throughput and sustainability were greatly enhanced by running the reaction as a slurry and decreasing the solvent to 2−5 volumes, and reducing enzyme loading to 20 wt % eliminated a cost barrier. However, less molnupiravir was obtained under these conditions and production plateaued at 70 LCAP under these conditions.

We sought better fundamental understanding of the reaction system in order to make further improvements. Monitoring the
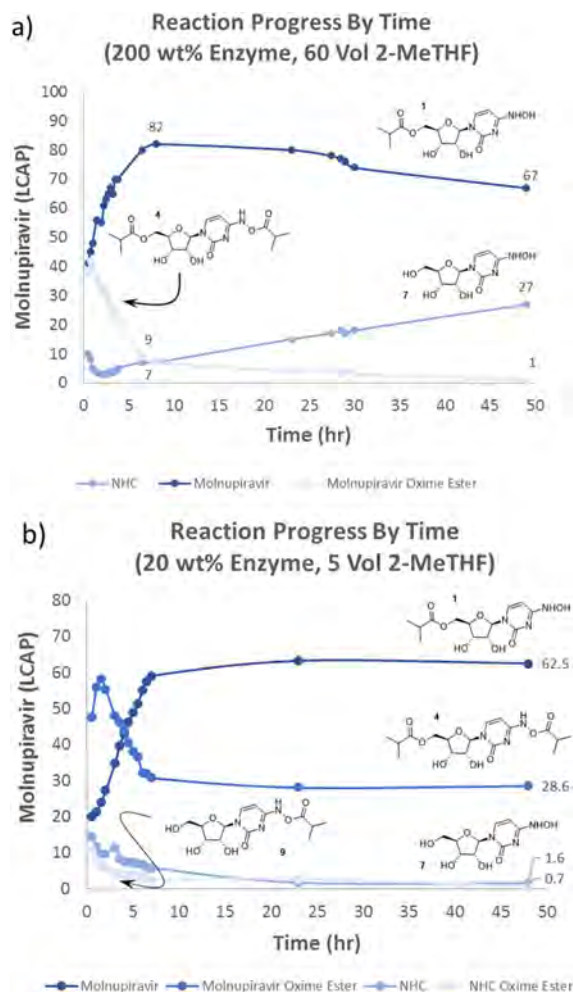
Figure 11. Reaction profile as a function of time shows unexpected trends in the impurity profile.

Figure 12. Postulated mechanism of esterification.

short-lived intermediate, **9**. This oxime ester is essentially an acyl-transfer reagent similar to acetone isobutyryl oxime ester. Following formation of the NHC oxime ester, a second esterification occurs, at the site of the primary alcohol to give a diacylated intermediate, molnupiravir isobutyryl oxime ester **4**. The oxime ester is then cleaved to give molnupiravir, **1**. Alternatively, the NHC isobutyryl oxime ester can be reverted to NHC. The primary alcohol is then acylated by either a second equivalent of oxime ester from acetone or from the NHC oxime ester to give molnupiravir The ester of molnupiravir can be cleaved to reform NHC, **7**, but this reaction is slower than cleavage of the oxime esters. We speculate that formation of the oxime ester is the kinetic but not thermodynamic product and that cleavage of oxime esters is the driving force of the reactions. Generation of acetone oxime is observed in the course of the reaction.

This hypothesis is supported by two additional observations (Figure 13). First, molnupiravir is formed when NHC isobutyryl

reaction as a function of time provided some of these insights (Figure 11). Several impurities were observed, identified, and tracked. The following conclusions emerged:

1. Molnupiravir reaches a maximum point at 8 h (84 LCAP), and then, the rate of degradation exceeds that of product formation. This results in decreasing levels of molnupiravir and increasing levels of NHC (Figure 11a).
2. NHC is mostly consumed with 3 h (3 LCAP); however, after this point, NHC levels begin to rise as it is regenerated (Figure 11a).
3. The over-acylated product **4**, molnupiravir isobutyryl oxime ester, is generated in large quantities early in the course of the reaction. This intermediate decays as the reaction progresses.
4. Smaller quantities of *N*-hydroxycytidine isobutyryl ester (**9**) are observed early in the reaction, and this intermediate also decreases with time (Figure 11b).
5. Using a lower enzyme loading results in a more stable reaction profile (Figure 11b).

It seems reasonable to postulate that the reaction is a series of equilibria based on acyl-transfer (Figure 12). Acylation of the *N*-hydroxy group appears to be fast and likely occurs first, forming a
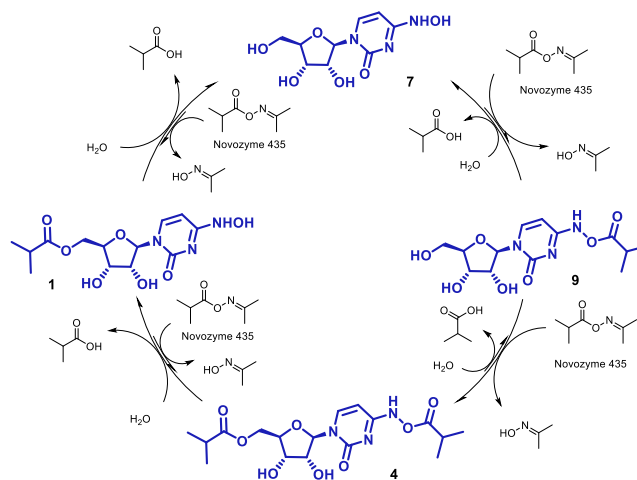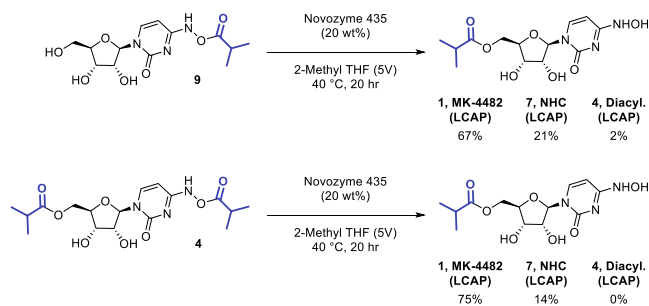

Figure 13. *N*-Hydroxycytidine oxime ester is labile, can be transferred to primary alcohol, and is cleaved in preference to ester.

oxime ester **9** is exposed to enzyme, even in the absence of acetone isobutyryl oxime ester, and no diacylated **4** is observed. Second, molnupiravir is again formed, when molnupiravir oxime ester **4** is in the presence of enzyme but in the absence of acetone isobutyryl oxime ester.

Initial exploration of purification conditions via crystallization revealed that the highly polar NHC was the most difficult impurity to purge. Based on the difficulty in rejecting NHC and the ease of eliminating the diacylated material, we surmised that it would be best to operate in a reaction regime that minimized the NHC content. Unfortunately, when NHC is minimized, the

reaction mixture has very high molnupiravir oxime ester levels (>20 LCAP), cutting into the reaction yield (Figure 11b).

Though the yield under these conditions appears low, we wondered whether the diacylated material could be directly converted to molnupiravir, thus increasing yield (Table 4). The

Table 4. Exploration of Ester Cleavage Reagents in Pursuit of Selective Cleavage of Oxime Ester
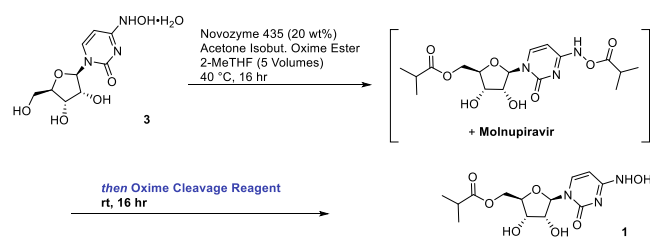
| entry	cleavage reagent	7, NHC (LCAP)	1, EIDD (LCAP)	4, diacyl. (LCAP)
1[a]		3	70	20
2	H_2O	3	71	19
3	MeOH	3	70	19
4	EtOH	4	69	19
5	NH_3 in EtOH	4	84	0
6	NH_4OH (aq.)	10	86	3
7	NH_2OH (aq.)	3	92	2

[a]Product distribution prior to addition of the cleavage reagent.

oxime ester bond seems to be easily cleaved. Probing this concept, a variety of oxime ester cleaving agents were added to molnupiravir oxime ester **4** to study material balance upon reaction. External alcohols showed little activity in cleaving the oxime ester (entries 1−3); however, nitrogenous additives showed substantial activity. Use of ammonia led to elevated levels of NHC, an undesired outcome. Selection of aqueous hydroxylamine was quite selective for reaction with oxime ester in preference to the primary ester (entry 7). In fact, the molnupiravir content increased from 66 LCAP to a value just over 92 LCAP.

Scale-up to 100 g. Possessing excellent reaction outcome, attention was turned to scale-up and isolation of the API from reaction solution (Figure 14). Water was the only solvent identified that purged NHC while affording sufficient recovery of the product. Fortunately, selection of water as a crystallization solvent for crude reaction mass returned material of excellent quality, and water did not cleave the ester to an appreciable extent. Examination of the mother liquor showed that some material was lost in filtration however (17.7%). This remains an opportunity for further improvement, and perhaps, the use of an antisolvent or salting effects will improve recovery. The overall yield of reaction was 93% with an isolated yield of 71%. The reaction was scaled two orders of magnitude to 100 g with very similar results.

CONCLUSIONS

In summary a practical, two-step route to molnupiravir from highly available cytidine was developed. The reaction features high yields and simple purification protocols, which can be performed at the scale. Reactions are run at high concentration with environmentally friendly solvents. Further room for improvements remains possible.
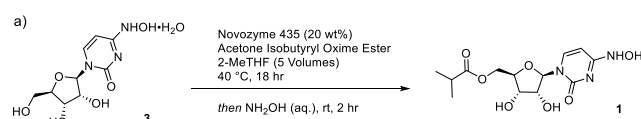
Entry	Scale (Input 3)	Before NH_2OH (1, 4, 7)	After NH_2OH (1, 4, 7)	Purity (qNMR, LCAP)	Yield
1	10 g	72.5, 20.6, 3.3	91.1, 2.5, 3.0	(100, 98.7)	67%
2	50 g	69.8, 22.8, 2.7	90.5, 2.8, 3.7	(99.5, 99.04)	68%
3	100 g	66.7, 28.5, 1.9	91.7, 3.0, 2.9	(100, 99.40)	71%

	MTBE (Filtrate)	Water (Mother Liquor)	Crystallized Solid	Total Mass
Mass, 1	5.10 g	21.1 g	84.3 g	110.5 g
Yield, 1	4.29%	17.7%	71.0%	93.0%

Figure 14. (a) Scale-up, (b) product distribution, and (c) mass balance for 100 g reaction.

EXPERIMENTAL SECTION

N-Hydroxycytidine Monohydrate (3). To a 2 L three-neck round-bottom flask equipped with an overhead stirrer and a J-KEM internal temperature probe, cytidine (500.00 g, 1.0 equiv, 2.056 mol), hydroxylamine sulphate (506.12 g, 1.5 equiv, 3.084 mol), and distilled water (1000 mL) was added. The mixture was stirred with 100 RPM and heated to 70 °C (internal temperature). The solid suspension was dissolved, and the reaction mixture became homogeneous after 10 min. The reaction mixture was stirred total for 5 h at the same temperature 70 °C (internal temperature). The reaction was monitored with HPLC, and 96% of cytidine was consumed. The heating was turned off, and the suspension was allowed to slowly cool to ambient temperature (25 °C) over the course of approximately 3 h, then cooled to an internal temperature −5 °C using an ice-salt bath, and stirred for additional 3 h. The solids were isolated by vacuum filtration through a Buchner funnel, washed with ice-cold water (500 mL × 3) and dried under vacuum oven (50 °C) for an overnight to afford a white crystalline solid with 84% yield (477.05 g), with 100% qNMR assay purity (mesitylene was used as the internal standard) and 100% by HPLC. ^{1}H NMR (600 MHz, CD$_3$OD): δ 7.18 (d, J = 8.4 Hz, 1H), 5.88 (d, J = 5.7 Hz, 1H), 5.62 (d, J = 8.3 Hz, 1H), 4.18 (t, J = 5.5 Hz, 1H), 4.13 (t, J =

4.7 Hz, 1H), 3.96 (d, J = 3.6 Hz, 1H), 3.80 (dd, J = 12.1, 2.9 Hz, 1H), 3.71 (dd, J = 12.1, 3.5 Hz, 1H) ppm. ^{13}C NMR (151 MHz, CD$_3$OD): δ 151.8, 146.3, 132.2, 99.3, 89.7, 86.1, 74.6, 71.74, 62.8 ppm. Data matched with those previously reported.[4a]

Acetone Isobutyryl Oxime Ester. To a 2 L three-neck round-bottom flask equipped with an overhead stirrer, a J-KEM internal temperature probe, and a nitrogen gas inlet, acetone oxime (100.0 g, 1.37 mol, 1.0 equiv), dichloromethane (1200 mL), and triethylamine (209.5 mL, 1.50 mol, 1.1 equiv) were added. The reaction mixture was stirred with 200 RPM and cooled to an internal temperature −5 °C using an ice-salt bath. Then, isobutyryl chloride (157.7 mL, 1.50 mol, 1.1 equiv) was added dropwise by maintaining an internal temperature below 0 °C. The reaction mixture was allowed to warm up to 20 °C (room temperature) and stirred for 16 h at the same temperature. The reaction mass was washed with H$_2$O (250 mL), 1 N HCl (250 mL), H$_2$O (250 mL), saturated solution of NaHCO$_3$ (250 mL), H$_2$O (250 mL), and brine solution (250 mL). The organic layer was dried over anhydrous Na$_2$SO$_4$, evaporated under vacuum in a rotavapor to give desired oxime ester as light-yellow oil (195 g, quantitative yield). ^{1}H and ^{13}C NMR data matched with those previously reported.[4a]

Molnupiravir (1). To a 1 L three-neck round-bottom flask equipped with an overhead stirrer, a J-KEM internal temperature probe, and a nitrogen gas inlet, N-hydroxycytidine hydrate (NHC.1H$_2$O; 100.00 g, 360.71 mmol, 1.0 equiv), oxime ester (154.94 g, 1.08 mol, 3.0 equiv), 2-methyltetrahydrofuran (500 mL), and NOVO enzyme-435 10,000 U/G (20.0 g, 20 wt %) were added in sequence. The mixture was stirred with 50 RPM and heated to 40 °C (internal temperature). The reaction was continued for 16 h at the same temperature. The reaction showed 1.9 LCAP for NHC, 66.7 LCAP for the product, and 29.5 LCAP for the diacylated product in HPLC at 260 nm. The heating was turned off, and the reaction mixture was allowed to cool to ambient temperature (25 °C). The reaction mass was filtered through the Buchner funnel to separate enzyme from the reaction mixture, and the enzyme was washed with 2-methyltetrahydrofuran (2 × 200 mL). The combined organic layer was transferred to a 2 L round-bottom flask, and hydroxylamine 50% in water (13 mL, 212.82 mmol, 0.59 equiv; approx. 2.0 equiv of the diacylated product) was added. The mixture was stirred at 20 °C (internal temperature) for 2 h. The HPLC analysis showed 2.9 LCAP for NHC, 91.7 LCAP for the product, and 3.0 LCAP for the diacylated product in the reaction mixture. The solvent was removed under reduced pressure, and methyl *tert*-butylether (MTBE; 1500 mL) was added and stirred at room temperature (20 °C) for 5 h. The reaction mass was filtered through a Buchner funnel and washed with MTBE (2 × 200 mL). The obtained solid was transferred to a 500 mL round-bottom flask equipped with an overhead stirrer and a J-KEM internal temperature probe, and water (250 mL) was added. The suspension was stirred with 50 RPM and heated at 70 °C (internal temperature) to get a clear solution (approx. 30 min). The solution was allowed to cool to room temperature (20 °C) and stirred (50 RPM) for overnight (16 h). The solids were collected by filtration through a Buchner funnel, washed with ice-cold water (2 × 200 mL), and dried under vacuum at 50 °C for an overnight to afford a white solid product with 71% yield (84.31 g), 100% qNMR assay purity (mesitylene was used as the internal standard), and 99.4% by HPLC. ^{1}H NMR (600 MHz, CD$_3$OD): δ 6.91 (d, J = 8.4 Hz, 1H), 5.82 (d, J = 4.8 Hz, 1H), 5.62 (d, J = 8.2 Hz, 1H), 4.29 (d, J = 3.6 Hz, 2H), 4.14 (t, J = 4.9 Hz, 1H), 4.10−4.07 (m, 2H), 2.62 (hept, J = 6.9 Hz, 1H),

1.18 (d, J = 7.0 Hz, 6H) ppm. ^{13}C NMR (151 MHz, CD$_3$OD): δ 178.3, 151.5, 146.1, 131.7, 99.5, 90.4, 82.6, 74.4, 71.5, 64.9, 35.1, 19.34, 19.33 ppm. Data matched with those previously reported.[4a]

■ ASSOCIATED CONTENT

ⓈI Supporting Information

The Supporting Information is available free of charge at https://pubs.acs.org/doi/10.1021/acs.oprd.1c00033.

> Reaction optimization, experimental details, and compound data (PDF)

■ AUTHOR INFORMATION

Corresponding Author

David R. Snead − *Medicines For All Institute, Richmond, Virginia 23298, United States;* ⓞ orcid.org/0000-0003-1239-533X; Email: drsnead@vcu.edu

Authors

Dinesh J. Paymode − *Medicines For All Institute, Richmond, Virginia 23298, United States;* ⓞ orcid.org/0000-0001-9059-6992

N. Vasudevan − *Medicines For All Institute, Richmond, Virginia 23298, United States*

Saeed Ahmad − *Medicines For All Institute, Richmond, Virginia 23298, United States*

Appasaheb L. Kadam − *Medicines For All Institute, Richmond, Virginia 23298, United States;* ⓞ orcid.org/0000-0002-0452-2901

Flavio S.P. Cardoso − *Medicines For All Institute, Richmond, Virginia 23298, United States;* ⓞ orcid.org/0000-0002-8608-5054

Justina M. Burns − *Medicines For All Institute, Richmond, Virginia 23298, United States*

Daniel W. Cook − *Medicines For All Institute, Richmond, Virginia 23298, United States;* ⓞ orcid.org/0000-0003-0621-3624

Rodger W. Stringham − *Medicines For All Institute, Richmond, Virginia 23298, United States*

Complete contact information is available at:
https://pubs.acs.org/10.1021/acs.oprd.1c00033

Author Contributions

D.J.P. and N.V. contributed equally and conducted chemical development work toward NHC and MK-4482. S.A. conducted market research on cytidine. A.L.K. prepared substrates for mechanistic studies. F.S.C.P. aided studies toward purification MK-4482. J.M.B., D.W.C., and R.W.S. developed analytical HPLC methods for NHC and MK-4482. D.R.S. guided research.

Notes

The authors declare no competing financial interest.

and Virginia General Assembly Higher Education Equipment Trust Fund (HEETF) to VCU.

■ REFERENCES

(1) Sheahan, T. P.; Sims, A. C.; Zhou, S.; Graham, R. L.; Pruijssers, A. J.; Agostini, M. L.; Leist, S. R.; Schäfer, A.; Dinnon, K. H., III; Stevens, L. J.; Chappell, J. D.; Lu, X.; Hughes, T. M.; George, A. S.; Hill, C. S.; Montgomery, S. A.; Brown, A. J.; Bluemling, G. R.; Natchus, M. G.; Saindane, M.; Kolykhalov, A. A.; Painter, G.; Harcourt, J.; Tamin, A.; Thornburg, N. J.; Swanstrom, R.; Denison, M. R.; Baric, R. S. An orally bioavailable broad-spectrum antiviral inhibits SARS-CoV-2 in human airway epithelial cell cultures and multiple coronaviruses in mice. *Sci. Transl. Med.* **2020**, *12*, eabb5883.

(2) Cox, R. M.; Wolf, J. D.; Plemper, R. K. Therapeutically administered ribonucleoside analogue MK-4482/EIDD-2801 blocks SARS-CoV-2 transmission in ferrets. *Nat. Microbiol.* **2021**, *6*, 11−18.

(3) (a) Salganik, R. I.; Vasjunina, E. A.; Poslovina, A. S.; Andreeva, I. S. Mutagenic action of N4-hydroxycytidine on Escherichia coli B cyt⁻. *Mutat. Res.* **1973**, *20*, 1−5. (b) Halford, B. An emerging antiviral takes aim at COVID-19. *Chem. Eng. News* **2020**, *98*, 22. (c) Cross. Merck & Co. joins race for COVID-19 vaccines and therapies. *Chem. Eng. News* **2020**, *98*, 12.

(4) (a) Vasudevan, N.; Ahlqvist, G. P.; McGeough, C. P.; Paymode, D. J.; Cardoso, F. S. P.; Lucas, T.; Dietz, J.-P.; Opatz, T.; Jamison, T. F.; Gupton, F. B.; Snead, D. R. A concise route to MK-4482 (EIDD-2801) from cytidine. *Chem. Commun.* **2020**, *56*, 13363−13364. (b) Gopalsamuthiram, V.; Williams, C.; Noble, J.; Jamison, T. F.; Gupton, B. F.; Snead, D. R. A Concise Route to MK-4482 (EIDD-2801) from Cytidine: Part 2. *Synlett* **2020**, *31*. (c) Steiner, A.; Znidar, D.; Ötvös, S. B.; Snead, D. R.; Dallinger, D.; Kappe, C. O. A High-Yielding Synthesis of EIDD-2801 from Uridine. *Eur. J. Org. Chem.* **2020**, 6736−6739. Note: The following report on chemical development of the same transformations conducted in the opposite order was published concurrently with this communication (d) Ahlqvist, G. P.; McGeough, C. P.; Senanayake, C.; Armstrong, J. D.; Yadaw, A.; Roy, S.; Ahmad, S.; Snead, D. R.; Jamison, T. F. Progress Toward a Large-Scale Synthesis of Molnupiravir (MK-4482, EIDD-2801) from Cytidine. *ACS Omega* **2021**, *6*, 10396−10402.

(5) (a) Painter, G.R.; Bluemling, G.R.; Natchus, M.G.; Guthrie, D. N4-hydroxycytidine and derivatives and anti-viral uses related thereto. WO2019113462, 2018. (b) Painter, G.R.; Perryman, D.; Bluemling, G.R. 4′-halogen containing nucleotide and nucleoside therapeutic compositions and uses related thereto. WO2019173602, 2019.

(6) Data taken from analysis of India import/export records.

(7) Benkovics, T.; McIntosh, J.; Silverman, S.; Kong, J.; Maligres, P.; Itoh, T.; Yang, H.; Huffman, M.; Verma, D.; Pan, W.; Ho, H.-I.; Vroom, J.; Knight, A.; Hurtak, J.; Morris, W.; Strotman, N.; Murphy, G.; Maloney, K.; Fier, P. Evolving to an Ideal Synthesis of Molnupiravir, an Investigational Treatment for COVID-19. *ChemRxiv* **2020** posted on 12/22/2020. DOI: 10.26434/chemrxiv.13472373.v1.

(8) (a) Morell, S.A.; Lipton, S.H.; Alexander, F. Process for the production of nucleotides. US2844514, 1958. (b) Einosuke, O.; Koichi, O.; Yukio, S.; Seizi, I.; Masahiko, Y.; Yoshio, N.; Ikuo, S. Production of 5′-nucleotides and of nucleosides. US3168446, 1965. (c) Yoshio, T.; Tadao, T.; Tetsuya, K.; Hisao, M.; Masaharu, Y.; Takehiko, I. Method of preparing 5′-ribonucleotides. US3201388, 1965. (d) Jingkang, Z. Process for preparing cytidine-S′-phosphate. CN1271080, 2006. (e) Zhang, J.; Ding, N.; Liu, Y. Method for preparing 5′-cytidylic acid from composite solvent and bind acid agent. CN102212096, 2011.

(9) (a) Suzuoki, Z.; Akira, K.; Katsuharu, Y. Dairy products. US3231385, 1966. (b) Gil, A.; Valverde, L. Nucleotide enriched humanized milk and process for its preparation. US4544559, 1981. (c) Ogoshi, S. Compositions of nucletic acid components for nutritional replenishment. US4758553, 1988. (d) Leary, H.L.; Burns, R.A. Nutritional formulas supplemented with nucleotides, and processes thereof. WO1998006277, 1998. (e) Masor, M.L.; Leach, J.L.; Molitor, B.E.; Benson, J.D.; Baxter, J.H. Infant nutritional formula with ribo-nucleotides. US5492899, 1996. (f) Masor, M.L.; Leach, J.L.; Molitor, B.E.; Benson, J.D.; Baxter, J.H. Nutritional formula with ribo-nucleotides. US5700590, 1997.

(10) Kinichiro, S.; Masajiro, K.; Akira, K. Process for improving the flavor of foods by the addition of 5′-nucleotides. US3104171, 1963.

(11) (a) Bobby, A.H.; Eugene, L.S. Dog food compositions. GB1200582, 1970. (b) Hamada, Y.; Yoshino, M. Nutrient ration for increasing growth of livestock and poultry. US3686392, 1972. (c) Shinzato, I.; Sato, H.; Toride, Y.; Takeuchi, M. Feed for livestock. US6777396, 2002. (d) Van de Ligt, C.P.A.; Cook, D.A.; Newcomb, M.D. Animal feed composition. US7326424, 2008. (e) Jiadong, C.; Xiaochun, C.; Xiaoquan, H.; Shuya, L.; Bing, S.; Yiwen, T.; Lei, Z. Weaned piglet nucleotide feed additive. CN102987169, 2013.

(12) (a) Bergmeyer, H.; Haid, E.; Nelboeck, H.M.; Weimann, G. Process for the preparation of nucleoside diphosphate esters. US3787392, 1974. (b) Leishan, C.; Liping, S.; Yan, W.; Ran, X. Citicoline and synthesizing method of citicoline not using phosphocholine chloride calcium. CN105693798, 2016.

(13) Communicated in private correspondence. Contact corresponding author if help is needed connecting with potential cytidine suppliers.

(14) Yongjun, L.; Guang, Y.; Jian, Z.; Jun, Z.; Weiqi, Z. A kind of Enzyme catalyzed synthesis technique of 5′ cytidine monophosphate. CN107365812, 2017.

(15) Li, F.; Xiong, Y. Novel method for synthesizing uridine. CN101717420, 2010.

(16) Asahi, S.; Tsunemi, Y.; Doi, M. Method for production of cytidine and/or deoxycytidine. US4839285, 1989.

(17) Tsunemi, Y.; Asahi, S.; Doi, M. Production of uridine. US4880736, 1989.

(18) (a) Henning, G. Improvements in and relating to processes for the production of nucleosides. GB486366, 1938. (b) Henning, G. Process for the preparation of nucleosides. CH215401, 1941.

(19) Chen, N.; Fan, X.; Ge, Y.; Hu, C.; Li, Y.; Ma, Q.; Song, X.; Wu, S.; Xie, X.; Xu, Q.; Zhang, C. Method for the enzymatic production of uridine monophosphate and cytidine monophosphate. AU2019101117, 2020.

(20) (a) Kinichiro, S.; Akira, K. Production of 5′-nucleotides. US3223592, 1965. (b) Louis, L.; Sidney, G. Enzyme digestion of nucleic acid. US3303100, 1967. (c) Doncheck, J.A.; Millis, J.R.; Swanson, P.E. Extraction of thymidine and other nucleosides. US5204245, 1993.

(21) (a) Brown, D. M.; Hewlins, M. J. E.; Schell, P. The tautomeric state of N(4)-hydroxy- and of N(4)-amino-cytosine derivatives. *J. Chem. Soc.* **1968**, 1925−1929. (b) Lee, G. C. Y.; Prestegard, J. H.; Chan, S. I. Tautomerism of nucleic acid bases. I. Cytosine. *J. Am. Chem. Soc.* **1972**, *94*, 951−959.